Variable Spin Iron(III) Chelates with Hexadentate Ligands Derived from Triethylenetetramine and Various Salicylaldehydes. Synthesis, Characterization, and Solution State Studies of a New $^2T \rightleftharpoons {}^6A$ Spin Equilibrium System[1]

Michael F. Tweedle[2] and Lon J. Wilson*

Contribution from the Department of Chemistry, William Marsh Rice University, Houston, Texas 77001. Received September 25, 1975

Abstract: Twelve new magnetically anomalous iron(III) complexes containing hexadentate ligands derived from triethylenetetramine (trien) and various X-substituted salicylaldehydes (X = H, NO_2, OCH_3), viz., [Fe(X-Sal$_2$trien)](Y) with Y^- = PF_6^-, NO_3^-, BPh_4^-, I^-, and Cl^-, have been synthesized and studied. In *solution*, the complexes are hexacoordinate, uni-univalent electrolytes which exhibit variable temperature magnetic susceptibility, ^1H NMR, and electronic spectral properties commensurate with a $^2T \rightleftharpoons {}^6A$ spin equilibrium with iron(III) in a tetragonally distorted ligand field environment. Thus, these complexes are the first synthetic iron(III) $^2T \rightleftharpoons {}^6A$ species reported to be completely devoid of Fe–S bonding. In general, electronegative NO_2 substituents favor the low-spin ^2T state and OCH_3 groups favor the high-spin ^6A state relative to the unsubstituted parent compound. For the parent [Fe(Sal$_2$trien)](Y) series, the $^2T \rightleftharpoons {}^6A$ equilibrium is strongly solvent dependent but essentially anion independent. The solvent dependency has been interpreted as arising mainly from a specific {[Fe(Sal$_2$trien)]$^+$·solvent} hydrogen bonding interaction involving the N–H protons on the trien backbone, where the strongest [N–H···solvent] hydrogen bonding produces the largest low-spin isomer population. Laser Raman temperature-jump kinetic measurements, performed in collaboration with Dr. Norman Sutin, yield dynamic spin state lifetimes for the [Fe(Sal$_2$trien)](PF$_6$) salt in methanol of $\tau(^2T) = 7.1 \times 10^{-8}$ s and $\tau(^6A) = 6.7 \times 10^{-8}$ s at 293 K and $\tau(^2T) = 1.2 \times 10^{-7}$ s and $\tau(^6A) = 1.1 \times 10^{-7}$ s at 277 K. Variable temperature magnetic susceptibility and Mossbauer spectroscopy measurements on the [Fe(Sal$_2$trien)](PF$_6$) complex have also been used to characterize the $^2T \rightleftharpoons {}^6A$ spin equilibrium in the *solid* state and to estimate the spin state lifetimes as being $\gtrsim 10^{-7}$ s for $T < 200$ K, assuming a dynamic $^2T \rightleftharpoons {}^6A$ process is also operative in the solid.

Metal complexes exhibiting spin equilibria between low-spin (ls) and high-spin (hs) electronic ground states have been recognized since Cambi, Siego, and Cagnasso first observed "magnetic isomerism" for the tris(dithiocarbamato)iron(III) complexes in 1931.[3] Since then, a number of other spin equilibrium systems of six-coordinate Fe(III), Fe(II), and Co(II) have also been studied, most of them within the past 15 years.[4] Usually these studies have focused upon the anomalous magnetic behavior in the *solid* state that accompanies the spin interconversion process in the crossover region where electron spin pairing and ligand field splitting energies are competitive. Very few of these studies, however, have also been concerned with the *solution* state. In fact, only the tris(dithiocarbamato)iron(III) series,[5] a [bis(*N,N*-disubstituted dithiocarbamato)dithiolene]iron(III ↔ IV) species,[6] a poly(1-pyrazolyl)borate iron(II) complex,[7] the [Fe^{II}(6-MePy)$_n$-(Py)$_m$trien]$^{2+}$ series,[8] and the bis(terpyridyl)cobalt(II) cation[9] have also been shown to exhibit the spin equilibrium phenomenon in solution. Since little is yet known about the chemical or electronic properties of variable spin species in solution, we have initiated efforts designed to systematically extend such investigation into the solution state for the purpose of (1) factoring-out unpredictable lattice effects such as phase changes, polymorphism, solvents of hydration, metal–metal interactions, etc., that can obscure the true electronic structure of the spin equilibrium phenomenon, (2) obtaining and interpreting kinetics for *intra*molecular (ls) $\rightleftharpoons$ (hs) spin interconversion processes in terms of metal ion electronic structure and ligand environment, and (3) measuring experimentally the role and energetics of spin multiplicity changes on chemical[10] and electrochemical[11] outer-sphere electron transfer processes. Such studies seem pertinent not only to inorganic systems involving electron spin changes, e.g., virtually all six-coordinate Co(II) (hs) ↔ Co(III) (ls) exchange couples,[12] but may also ultimately aid in understanding biochemical electron transport patterns of redox-active variable-spin metalloproteins.[13,14]

In an initial attempt to develop solution-stable spin equilibrium systems for study, we recently reported a series of Fe(II) complexes derived from the hexadentate ligands, tris{4-[(6-R)-2-pyridyl]-3-aza-3-butenyl}amines, where R = H or CH$_3$.[8] The Fe(II) complexes, as PF$_6^-$ salts, are shown in Figure 1 along with their ligand abbreviations. In solution, the four derivatives were found to exhibit varied magnetic behavior depending on the R substitution pattern with [Fe(Py$_3$tren)]$^{2+}$ being low-spin (^1A ground state) and [Fe(6-MePy)$_3$tren]$^{2+}$ high-spin (^5T ground state) over a 250° temperature range. More interesting, however, both the [Fe(6-MePy)(Py)$_2$tren]$^{2+}$ and [Fe(6-MePy)$_2$(Py)tren]$^{2+}$ derivatives were found to display anomalous magnetic behavior typically found for an $^1A \rightleftharpoons {}^5T$ spin equilibrium process. Thus, these complexes, along with the iron(II) poly(1-pyrazolyl)borates are among the first Fe(II) complexes found to support spin equilibria in solution as well as in the solid state.

As found for the [Fe(6-MePy)$_n$(Py)$_m$tren]$^{2+}$ series, hexadentate ligands offer several distinct advantages as chelating agents in the design of variable spin systems for solution studies: (1) the "chelate effect" apparently aids in producing solution-stable species, avoiding disproportion reactions which can occur for lesser dentate complexes, e.g., [Fe(phen)$_2$Cl$_2$] (hs, solid) + solvent → [Fe(phen)$_3$]$^{2+}$ (ls, solution), (2) ligand substituent effects permit a gradual and systematic "fine-tuning" of the ligand field strength in the crossover region, and, most importantly, (3) coordinately saturated complexes with a single hexadentate ligand should promote only outer-sphere electron transfer processes, making mechanistic interpretation of any electron transfer kinetics more straight-forward. In the present work, we wish to report the solution state properties of new Fe(III) spin equilibrium complexes of the hexadentate ligands derived from triethylenetetramine (trien) and various X-substituted salicylaldehydes (X-Sal), as shown in Figure 2. In solution, the [Fe(X-Sal$_2$trien)]$^+$ complexes exhibit variable temperature magnetic, electronic spectral, and ^1H
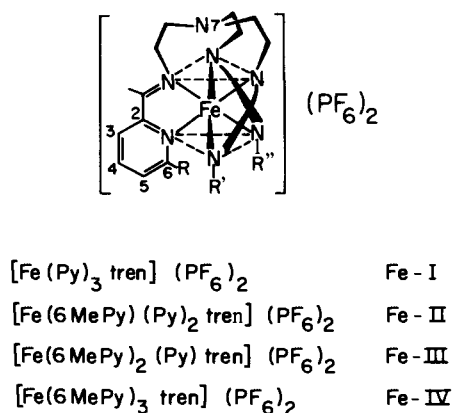
Figure 1. Structure of the $[Fe(6MePy)_n(Py)_m tren](PF_6)_2$ complexes.

$$[Fe(Py)_3 tren] (PF_6)_2 \qquad Fe - I$$

$$[Fe(6MePy)(Py)_2 tren] (PF_6)_2 \qquad Fe - II$$

$$[Fe(6MePy)_2(Py) tren] (PF_6)_2 \qquad Fe - III$$

$$[Fe(6MePy)_3 tren] (PF_6)_2 \qquad Fe - IV$$

NMR properties commensurate with a $^2T(ls) \rightleftharpoons {}^6A(hs)$ spin equilibrium for Fe(III) in a tetragonally distorted octahedral ligand field environment. Systematic control of the spin equilibria in solution has been accomplished and understood in terms of a combined ligand substituent and solvent effect. Finally, the laser Raman temperature-jump technique developed at Brookhaven[15] has been used to directly measure the dynamic spin state lifetimes, $\tau(^2T)$ and $\tau(^6A)$, in methanol solution for the parent $[Fe(Sal_2trien)](PF_6)$ complex.

Experimental Section

Physical Measurements. Magnetic susceptibilities in the solid state were measured by the Faraday technique using $Hg[Co(NCS)_4]$ as the calibrant. Pascal constants were used to correct for water, ligand, and anion diamagnetism: Sal_2trien, -171×10^{-6}; x-OCH_3Sal_2trien, -207×10^{-6}; x-NO_2Sal_2trien, -200×10^{-6}; PF_6^-, -64.1×10^{-6}; BPh_4^-, -220×10^{-6}; NO_3^-, -19×10^{-6}; Cl^-, -23×10^{-6}; I^-, -51×10^{-6}; H_2O, -13×10^{-6} cgs. Measurements in solution were performed by the Evans ^1H NMR method.[16] A methanol sample was used for temperature calibration. The measurements were corrected for changes in solvent density and sample concentration with temperature.[17] Where possible, both chloroform and Me_4Si were used as inert reference compounds, with both giving identical ^1H NMR splittings and, thus, identical calculated moments; solvent proton signals could not be used for the magnetic moment calculations since these splittings differed substantially from the reference compound splittings.

Solid and solution state infrared spectra were obtained on a Beckman IR-20 using KBr plates and Nujol mulls for the solids and Beckman IR-Tran2 cells for the solutions. Solution conductivities were obtained using a Model 31 YSI conductivity bridge. ^1H NMR spectra were run at 60 MHz on a Perkin-Elmer R12 or Varian A-56/60A spectrometer and calibrated using the conventional sideband technique. Uv-visible spectra were run on a Cary 17 instrument using jacketed, insulated quartz cells; sample temperatures were monitored using a thermistor. Electrochemical measurements were obtained in $\sim 10^{-3}$ M acetone solutions (0.1 M TEAP) at room temperature using a PAR Model 174 polarographic analyzer equipped with a dropping mercury electrode assembly. Mossbauer spectra were run on an apparatus already described,[18] but modified to include an Elron Mossbauer function generator and transducer drive assembly and a Packard 1024 channel analyzer. Mossbauer spectra were computer analyzed using the program of Chrisman and Tumolillo.[19]

The temperature-jump experiments were performed using the laser stimulated Raman system previously described.[15] For the experiments, sample cells with 0.020–0.81 mm path lengths were employed. Methanol was used a solvent, and data were obtained at 4 and 20 °C in thermostated cells (±2 °C). The relaxation traces obtained from photographs of oscilloscope traces measured the change in optical density of the sample spectrum with time at 20 410 cm^{-1}. The first-order relaxation time, τ in nanoseconds, for the

$$^2T(Fe^{3+}, ls) \underset{k_{-1}}{\overset{k_1}{\rightleftharpoons}} {}^6A(Fe^{3+}, hs)$$
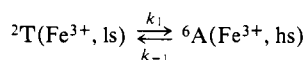
spin interconversion process was determined from log $(I_\infty - I)$ vs. time
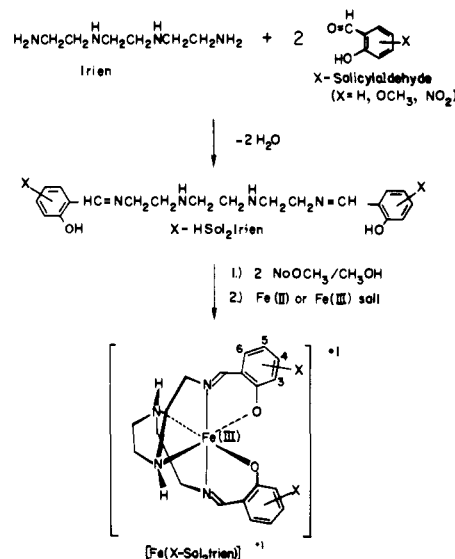

Figure 2. Synthesis and structure of the $[Fe(X-Sal_2trien)]^+$ complexes.

plots generated from the photographs. Equilibrium constants, $K_{eq} = k_1/k_{-1}$, were obtained from the magnetic susceptibility measurements, with the values used being 0.89 at 4 °C and 1.03 at 20 °C for the $[Fe(Sal_2trien)](PF_6)$ compound in methanol. Rate constants, k_1 and k_{-1}, were calculated from the measured relaxation times of $\tau = 35 \pm 8$ ns at 20 °C and 60 $\pm$ 15 ns at 4 °C and the equilibrium constants from the relationship, $\tau = (k_1 + k_{-1})^{-1}$. The spin state lifetime τ (spin state), is then k^{-1}.

Materials and Syntheses. Recrystallized grade triethylenetetramine tetrahydrochloride (trien·4HCl) and salicylaldehydes from Aldrich or Eastman Kodak were used as received. Spectroquality acetone, MeOH and DMF, and reagent grade CH_3CN, pyridine, Me_2SO, and HMPA were used for the ir and ^1H NMR studies without further purification; practical grade CH_3NO_2 and $C_6H_5NO_2$ were used with the $C_6H_5NO_2$ being purified prior to use. Chemical analyses were by the microanalytical laboratory of the School of Chemical Sciences, University of Illinois, and by Galbraith Analytical Laboratories, Knoxville, Tenn.

Isolation of Triethylenetetramine (trien). Trien·4HCl (14.6 g, 50 mmol) was dissolved in 50 ml of water, to which a 40% aqueous solution of NaOH was added, with stirring, until an orange-yellow oil separated. The trien oil was extracted into dry chloroform and the solution reduced in volume under reduced pressure at room temperature. The trien oil which remained was used without further treatment. Yield: 4.5–6.0 g, 60–80%.

[Fe(Sal$_2$trien)](PF$_6$) was prepared by adding trien (1.46 g, 10 mmol)· dissolved in 10 ml of methanol to a stirring solution of salicylaldehyde (2.44 g, 20 mmol) in 40 ml of methanol. The solution turned yellow immediately and was allowed to stir at room temperature for 10 min. To this stirring solution, 1.08 g (20 mmol) of NaOCH$_3$ dissolved in 50 ml of methanol was added slowly. Finally, a 50-ml methanol solution containing Fe(NO$_3$)$_3$·9H$_2$O (4.04 g, 10 mmol) was added dropwise to the ligand solution, producing a solution which was dark purple in color. The solution was filtered and taken to dryness under reduced pressure at room temperature. The solid residue was extracted into 200 ml of warm water. Addition of KPF$_6$ (7.6 g, 40 mmol) dissolved in 100 ml of water resulted in the initial formation of a brown precipitate. Cooling and reduction of the solution volume to approximately 150 ml produced a brown solid which was collected by filtration and washed with water. The brown solid was recrystallized twice from an acetone–water solution (approximately 70:30 by volume) by cooling with volume reduction under reduced pressure. The resulting shiny black crystals were washed with water, then ether, and dried under vacuum at 117 °C over P$_2$O$_5$ for 12 h. Yield: 2.2 g, 50%. The compound is reversibly thermochromic in solution, changing, for example, from reddish purple at room temperature to blue by -80 °C in acetone.

[Fe(Sal$_2$trien)](NO$_3$)·1.5H$_2$O was prepared as described above for the PF$_6^-$ salt except that KPF$_6$ was not added. Rather, the 200 ml aqueous solution was reduced in volume under reduced pressure with

cooling until crystallization occurred. Upon cooling at 0 °C for 10 h, hexagon-shaped black crystals were obtained. The crystals were recrystallized from 125 ml of warm water by repeating the above cooling and concentrating procedure, then dried under vacuum at room temperature over P_2O_5 for 12 h. Yield: 1.20 g, 25%. The compound is reversibly thermochromic in solution, changing, for example, from reddish purple at room temperature to blue by −80 °C in methanol.

[Fe(Sal$_2$trien)](BPh$_4$) was prepared by metathesis from the NO$_3^-$ salt. To 0.32 g (0.64 mmol) of the NO$_3^-$ salt dissolved in 30 ml of warm water was added 20 ml of an aqueous solution containing 0.32 g (1 mmol) of NaBPh$_4$. The brown solid that precipitated was collected by filtration and recrystallized from an acetone-ether (1:3 by volume) solution with cooling. The resulting crystals were crushed into a fine powder and dried under vacuum at 117 °C over P_2O_5 for 24 h. (Note: The compound must be dried as a fine powder to remove acetone which tends to occlude as a solvent of crystallization.) Yield 0.29 g, 90%. In methanol, the compound exhibits the same thermochromism as the NO$_3^-$ salt.

[Fe(Sal$_2$trien)]I·H$_2$O was prepared by metathesis from the NO$_3^-$ salt. To 0.50 g (1.02 mmol) of the NO$_3^-$ salt dissolved in 25 ml of warm water was added 25 ml of an aqueous solution saturated in NaI at room temperature. Black crystals were obtained by cooling the solution in an ice bath for ~2 h. The crystals were recrystallized and dried as above for the BPh$_4^-$ salt. Yield: 0.20 g, 40%. In acetone, the compound exhibits the same thermochromism as does the PF$_6^-$ salt.

[Fe(Sal$_2$trien)]Cl·2H$_2$O was prepared by metathesis from the PF$_6^-$ salt. To 1.10 g (2 mmol) of the PF$_6^-$ salt dissolved in 30 ml of acetone was added 75 ml of an acetone solution containing 0.32 g (8 mmol) of LiCl. The black solid that formed immediately was collected by filtration, washed with acetone, and dried under vacuum at room temperature over P_2O_5 for 12 h. Yield: 0.90 g, 95%. In methanol, the compound exhibits the same thermochromism as the NO$_3^-$ salt. Hydrated chloride salts of the other [Fe(X-Sal$_2$trien)]$^+$ compounds are also prepared from their PF$_6^-$ salts in a similar manner, and in similar yield.

[Fe(x-OCH$_3$Sal$_2$trien)](PF$_6$) for x = 3 or 5 was prepared as described above for the parent compound except that 3.04 g (20 mmol) of the appropriate x-OCH$_3$ salicylaldehyde was used. After the addition of the aqueous KPF$_6$ solution, the purple colored solution was taken to dryness under reduced pressure at room temperature. Extraction of the purple colored residue with 50 ml of dry acetone resulted in a purple solution from which dark purple crystals were obtained with cooling by the slow addition of ether over approximately 14 h. The product was recrystallized twice from an acetone-ether mixture (1:3 by volume), collected by filtration, washed with ether, and dried as above for the parent BPh$_4^-$ salt. Yield: 0.50 g, 10%. The compounds are reversibly thermochromic in solution, changing, for example, from deep purple at room temperature to emerald green by −100 °C in acetone.

[Fe(4-OCH$_3$Sal$_2$trien)](PF$_6$) was prepared by adding trien (0.73 g, 5 mmol), dissolved in 20 ml of methanol, dropwise to a stirring solution of 4-OCH$_3$ salicylaldehyde (1.52 g, 10 mmol) in 20 ml of methanol at 0 °C. To the resulting yellow solution, 0.64 g (10 mmol) of KOH in 10 ml of water was added first, followed by the slow dropwise addition of Fe(NO$_3$)$_3$·9H$_2$O (2.02 g, 5 mmol) dissolved in 50 ml of methanol. The resulting cherry red solution was concentrated to ca. half its original volume under reduced pressure and the small amount of white precipitate that formed was removed by filtration. Addition of KPF$_6$ (1.90 g, 10 mmol) in 50 ml of water resulted in the formation of a red precipitate after 10 min of stirring at room temperature. The red solid was collected by filtration and washed with cold water until the filtrate changed from dark red to light red in color. The solid was then washed with ether and recrystallized twice from CH$_2$Cl$_2$ with cooling and the slow addition of ether over a 20-h period. The resulting dark red needles were washed with cold water, then ether, and then dried as above for the parent PF$_6^-$ salt. Yield: 1.50 g, 50%. The compound is reversibly thermochromic in solution, changing, for example, from dark cherry red at room temperature to light red by −80 °C in acetone.

[Fe(x-NO$_2$Sal$_2$trien)](PF$_6$) with x = 3 or 5 was prepared by dissolving trien (1.70 g, 11.7 mmol) in 50 ml of methanol and slowly adding the appropriate x-NO$_2$ salicylaldehyde dissolved in 150 ml of methanol. After ca. two-thirds of the aldehyde solution had been added, a wet-looking orange precipitate formed. Upon cooling to 0

°C and with the addition of NaOCH$_3$ (1.30 g, 23.4 mmol) dissolved in 50 ml of methanol, most of the precipitate in the 3-NO$_2$ ligand solution dissolved to give an orange solution. For the 5-NO$_2$ ligand solution, KOH (1.50 g, ~27 mmol) dissolved in 10 ml of water was used as the base to give the same orange colored solution with a small amount of orange solid remaining in suspension. Upon addition of Fe(NO$_3$)$_3$·9H$_2$O (4.70 g, 11.7 mmol) dissolved in 35 ml of methanol, the solution turned brown (green-brown for 5-NO$_2$) and a brown solid precipitated. The solution was filtered and the solid residue washed with 100 ml of methanol. The residue which remained after the washing was discarded. To the brown filtrate, 50 ml of an aqueous solution of KPF$_6$ (7.6 g, 40 mmol) was added and the resulting solution cooled and concentrated under reduced pressure until crystallization occurred. The product was recrystallized from an acetone-ether solution at 0 °C and dried as above for the parent PF$_6^-$ salt. Yield: 3-NO$_2$, 1.20 g, 20%; 5-NO$_2$, 0.50 g, 12%. The compounds are reversibly thermochromic in solution with the 3-NO$_2$ derivative changing from reddish brown to purple and the 5-NO$_2$ derivative from red (transmitted light) or green (reflected light) to predominantly green (transmitted or reflected light) in going from room temperature to −80 °C in acetone.

[Fe(Sal$_2$trien-d_2)](PF$_6$) was prepared by dissolving a small amount of [Fe(Sal$_2$trien)]Cl·2H$_2$O in D$_2$O and allowing it to stand at room temperature for 12 h. Addition of a filtered D$_2$O solution of KPF$_6$ produced immediate precipitation of the deuterated N-D compound as the PF$_6^-$ salt in nearly quantitative yield. The compound was collected by filtration, washed with a small portion of D$_2$O, and dried as above for the undeuterated product. Deuteration was judged to be effectively complete as evidenced in the ir spectrum by the disappearance of the N-H(st) at 3310 cm^{-1} and the appearance of an N-D(st) at 2453 cm^{-1}. The relationship, $\nu_{N-H} = 1.36 \nu_{N-D}$, was empirically determined to be valid for both the solid and solution states. Both the N-D and N-H parent complexes were used whenever possible as a check during the solution ir studies. No base is needed to catalyze the deuterium exchange; in fact, as evidenced by solution ir studies, some exchange occurs within a few minutes at room temperature in deuterated solvents such as acetone-d_6, CD$_3$CN, and CD$_3$NO$_2$; in CD$_2$Cl$_2$ no exchange occurs over a period of 1-2 h. μ_{eff} (295 K, solid) = 5.93 μ_B.

Variable Temperature Susceptibility Data. [Fe(Sal$_2$trien)](PF$_6$) (solid): temperature = 293.5 K, χ_M' (corr) = 14 269 × 10^{-6} cgs mol^{-1}, μ_{eff} = 5.81 μ_B; 272.6, 13 340, 5.81; 253.4, 16 411, 5.79; 235.3, 17 518, 5.77; 217.0, 18 822, 5.74; 198.9, 20 221, 5.69; 181.0, 20 270, 5.44; 163.4, 20 349, 5.18; 145.9, 19 881, 4.84; 128.2, 18 900, 4.42; 111.8, 18 821, 4.12; 94.3, 20 556, 3.95; 82.8, 22 332, 3.86.

[Fe(Sal$_2$trien)](PF$_6$) (acetone): temperature = 326.2 K, χ_M' (corr) = 10 556 × 10^{-6} cgs mol^{-1}, μ_{eff} = 5.27 μ_B; 318.8, 10 556, 5.21; 301.7, 10 233, 4.99; 294.7, 10 060, 4.89; 279.2, 9072, 4.52; 258.0, 7650, 3.99; 250.2, 7351, 3.85; 241.1, 6192, 3.47; 226.0, 4970, 3.01; 219.2, 4277, 2.75; 213.0, 3437, 2.43; 204.8, 3011, 2.24; 194.8, 2623, 2.03; 186.4, 2326, 1.87; 181.2, 2342, 1.85.

[Fe(Sal$_2$trien)](PF$_6$) (methanol): temperature = 323.2 K, χ_M' (corr) = 9248 × 10^{-6} cgs mol^{-1}, μ_{eff} = 4.91 μ_B; 314.1, 9094, 4.80; 307.2, 9106, 4.75; 290.2, 8084, 4.35; 274.3, 7088, 3.96; 256.2, 6030, 3.53.

[Fe(Sal$_2$trien)](PF$_6$)$_2$(acetonitrile): temperature = 307.0 K, χ_M' (corr) = 10 259 × 10^{-6} cgs mol^{-1}, μ_{eff} = 5.04 μ_B; 281.0, 9788, 4.71; 261.5, 8443, 4.22; 242.6, 6771, 3.64.

[Fe(Sal$_2$trien)](PF$_6$) (pyridine): temperature = 307.0 K, χ_M' (corr) = 7748 × 10^{-6} cgs mol^{-1}, μ_{eff} = 4.38 μ_B; 281.0, 6849, 3.94; 261.5, 5546, 3.42; 242.0, 4045, 2.81.

[Fe(Sal$_2$trien)](PF$_6$) (acetone-water solution, 50:50 mole fraction measured by weight): temperature = 308.8 K, χ_M' (corr) = 8276 × 10^{-6} cgs mol^{-1}, μ_{eff} = 4.54 μ_B; 295.6, 7576, 4.25; 279.2, 6789, 3.91; 269.8, 5726, 3.53; 260.2, 5158, 3.29; 249.2, 3790, 2.76; 237.6, 3447, 2.57.

[Fe(Sal$_2$trien)](PF$_6$) (methylene chloride): temperature = 307.0 K, χ_M' (corr) = 11 820 × 10^{-6} cgs mol^{-1}, μ_{eff} = 5.41 μ_B; 269.0, 9417, 4.52; 210.0, 3839, 2.55; 182.5, 2453, 1.90.

[Fe(Sal$_2$trien-d_2)](PF$_6$) (methylene chloride): temperature = 307.0 K, χ_M' (corr) = 11 344 × 10^{-6} cgs mol^{-1}, μ_{eff} = 5.30 μ_B; 269.0, 9209, 4.47; 210.0, 3720, 2.51; 182.5, 2583, 1.95.

[Fe(3-OCH$_3$Sal$_2$trien)](PF$_6$) (acetone): temperature = 318.8 K, χ_M' (corr) = 10 966 × 10^{-6} cgs mol^{-1}, μ_{eff} = 5.31 μ_B; 294.7, 10 814, 5.07; 279.2, 10 662, 4.90; 258.0, 10 124, 4.59; 250.2, 9857, 4.46; 241.1, 9067, 4.20; 226.0, 7470, 3.69; 219.2, 6500, 3.39; 202.2, 4603, 2.74; 181.2, 3342, 2.21.

Table I. Analytical, Conductivity, and Single Temperature Magnetic Data for the [Fe(X-Sal$_2$trien)]$^+$ Complexes

Compound	Color[a]	Calcd, %			Found, %			Λ$_C$[b]	μ$_{eff}$ (μ$_B$) Solution 307 K[c]	Solid 295 K[d]
		C	H	N	C	H	N			
[Fe(Sal$_2$trien)]PF$_6$	Dark brown	43.42	4.37	10.13	43.14	4.47	10.01	150	5.05; 5.01 (CH$_3$CN)	5.81
[Fe(Sal$_2$trien)]NO$_3$·1.5H$_2$O	Black	48.30	5.47	14.08	48.14	5.46	14.31	134	4.97 (CH$_3$CN)	2.47
[Fe(Sal$_2$trien)]BPh$_4$	Dark brown	72.64	6.10	7.70	72.76	5.96	7.72	110 (CH$_3$CN)	5.16 (CH$_3$CN)	5.08
[Fe(Sal$_2$trien)]Cl·2H$_2$O	Blue-black	50.07	5.88	11.68	50.03	5.91	11.43	127 (CH$_3$CN)	4.93 (CH$_3$CN)	1.94
[Fe(Sal$_2$trien)]I·H$_2$O	Black	43.42	4.74	10.12	43.46	4.63	10.32	149 (CH$_3$CN)	4.94 (CH$_3$CN)	2.33
[Fe(3-OCH$_3$Sal$_2$trien)]PF$_6$	Black	43.09	4.60	9.14	43.34	4.53	8.72	159	5.22	5.86
[Fe(3-OCH$_3$Sal$_2$trien)]Cl·2H$_2$O	Green	48.95	5.97	10.38	48.52	5.63	10.21	126 (CH$_3$CN)	5.63 (CH$_3$CN)	2.45
[Fe(4-OCH$_3$Sal$_2$trien)]PF$_6$	Dark red	43.09	4.60	9.14	43.48	4.68	9.24	134	5.91	5.79
[Fe(5-OCH$_3$Sal$_2$trien)]PF$_6$	Black	43.09	4.60	9.14	43.47	4.75	8.79	152	5.59	5.81
[Fe(3-NO$_2$Sal$_2$trien)]PF$_6$	Brick red	37.35	3.45	13.07	37.24	3.50	12.86	149	4.40	5.66
[Fe(3-NO$_2$Sal$_2$trien)]Cl·H$_2$O	Red-brown	43.54	4.31	14.99	43.92	4.20	15.11	85 (CH$_3$OH)	4.32(CH$_3$OH)	4.82
[Fe(5-NO$_2$Sal$_2$trien)]PF$_6$·H$_2$O	Red-brown	36.32	3.66	12.71	36.09	3.60	12.75	145	3.15	5.07
[Fe(5-NO$_2$Sal$_2$trien)]Cl·H$_2$O	Brown	43.54	4.31	14.99	43.71	4.54	15.28	101 (CH$_3$OH)	2.93 (CH$_3$OH)	2.15

^{a} Microcrystalline sample. ^{b} μmho cm^{-1} at 30 C for 10^{-3} M acetone solutions except where indicated. Comparative values for 10^{-3} M (Et$_4$N)ClO$_4$ solutions of acetone, CH$_3$CN, and CH$_3$OH are 200, 192, and 125 μmho cm^{-1}, respectively. ^{c} Determined by the Evans method (chloroform reference) in ~10^{-2} M acetone solutions except where indicated; estimated maximum error: 0.10 μ$_B$. ^{d} Determined by Faraday method; estimated maximum error: 0.02 μ$_B$.

[Fe(4-OCH$_3$Sal$_2$trien)](PF$_6$) (acetone): temperature = 310.3 K, χ$_M'$ (corr) = 13 956 × 10^{-6} cgs mol^{-1}, μ$_{eff}$ = 5.91 μ$_B$; 299.2, 14 278, 5.87; 284.4, 13 477, 5.56; 273.2, 13 038, 5.36; 257.7, 11 932, 4.98; 249.2, 11 559, 4.82; 238.8, 10 843, 4.57; 227.9, 9505, 4.18; 223.2, 8799, 3.98; 211.0, 7489, 3.57; 200.7, 5486, 2.98; 192.2, 4228, 2.56.

[Fe(5-OCH$_3$Sal$_2$trien)](PF$_6$) (acetone): temperature = 314.2 K, χ$_M'$ (corr) = 12 821 × 10^{-6} cgs mol^{-1}, μ$_{eff}$ = 5.70 μ$_B$; 303.5, 12 629, 5.56; 286.9, 11 196, 5.09; 277.2, 10 651, 4.88; 262.2, 9876, 4.57; 255.9, 8834, 4.27; 241.6, 7217, 3.75; 233.7, 6169, 3.41; 224.2, 5314, 3.10; 214.2, 4538, 2.80; 199.2, 3706, 2.44; 190.2, 3271, 2.24; 183.2, 3042, 2.12.

[Fe(3-NO$_2$Sal$_2$trien)](PF$_6$) (acetone): temperature = 318.8 K, χ$_M'$ (corr) = 8301 × 10^{-6} cgs mol^{-1}, μ$_{eff}$ = 4.62 μ$_B$; 301.7, 7776, 4.35; 294.7, 7528, 4.23; 279.2, 6446, 3.81; 258.0, 5523, 3.39; 250.2, 5170, 3.23; 241.1, 4657, 3.01; 226.6, 3766, 2.62; 219.2, 3563, 2.51; 202.2, 3415, 2.36; 181.2, 3312, 2.20.

[Fe(5-NO$_2$Sal$_2$trien)](PF$_6$) (acetone): temperature = 321.8 K, χ$_M'$ (corr) = 4480 × 10^{-6} cgs mol^{-1}, μ$_{eff}$ = 3.41 μ$_B$; 310.4, 4142, 3.22; 299.2, 3705, 2.99; 284.4, 3297, 2.75; 273.1, 2815, 2.49; 257.7, 2457, 2.26; 249.2, 2173, 2.09; 238.8, 1954, 1.94; 228.0, 2005, 1.92; 206.7, 2423, 2.01.

Results and Discussion

Synthesis and Characterization of the [Fe(X-Sal$_2$trien)](Y) Complexes. As shown generally in Figure 2, the in situ synthesis for the series of X-HSal$_2$trien ligands (X = H, OCH$_3$, NO$_2$) is straightforward, involving a Schiff base condensation reaction of trien with the appropriate salicylaldehyde. A linear representation for the X-HSal$_2$trien ligand structure is likely an oversimplification, however, since salicylaldehyde is known to react with trien to give a trissalicylideneaminotriethylenetetramine compound,

$$HOC_6H_4CH=N(CH_2)_2N(CH_2)_2N(CH_2)_2N=CHC_6H_4OH$$
$$\overset{|}{CHC_6H_4OH}$$
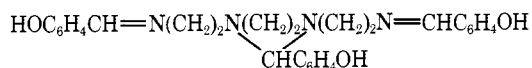
which can be isolated.[20] In the presence of base and metal ions, however, the central salicylaldehyde is liberated during the formation of hexadentate complexes. In fact, a crystal structure of the [Ni(Sal$_2$trien)]·6H$_2$O complex[21] has established that the mode of chelation for the Sal$_2$trien ligand with Ni(II) is not only hexadentate but also geometrically specific for the C$_2$ molecular geometry shown in the figure. This result is not surprising in view of the fact that space filling molecular models also indicate this to be the most strain-free geometry for the ligand to adopt when functioning in its fully hexadentate fashion. It is likely, therefore, that all the six-coordinate [M(Sal$_2$trien)]$^+$ complexes (M = Al(III), Co(III) and

Fe(III)), as first reported by Sarma and Bailar,[22] are of this same general geometry, possessing four five-membered chelate rings in the trien backbone and two six-membered rings of the salicylaldimine moieties. Magnetically, the most interesting member of the Sarma and Bailar series was the Fe(III) complex, [Fe(Sal$_2$trien)]I·1.5H$_2$O, which was reported to be low spin in the solid state with μ$_{eff}$ (300 K) = 1.81 μ$_B$.[22] Although a NO$_3$·1.5H$_2$O salt was also prepared, no magnetic data were reported and no characterization in solution was given for either [Fe(Sal$_2$trien)]$^+$ species. Because low-spin pseudooctahedral complexes of Fe(III) are relatively rare, and because of our interest in obtaining and studying spin equilibria of hexadentate ligand-containing complexes in solution, we were attracted to these [Fe(X-Sal$_2$trien)]$^+$ species. Our initial efforts have focused on the solution properties of the ^{2}T $\rightleftarrows$ ^{6}A spin equilibria found for the Fe(III) series, although a few preliminary solid state magnetic and Mossbauer data are also presented for completeness and for solution vs. solid state comparative purposes. A full solid state study of variable temperature and pressure magnetic, Mossbauer, infrared, ESCA, and x-ray structural properties for the series will be reported later.[23]

Table I contains analytical, solution conductivity, and single temperature magnetic moment data, in both solid and solution states, used to characterize the new [Fe(X-Sal$_2$trien)](Y) complexes. Taken together, the conductivity and analytical data are consistent with the proposed molecular formulation for the [Fe(X-Sal$_2$trien)](Y) salts as being uni-univalent electrolytes in solution with the Fe(III) complex cation having the general six-coordinate structure shown in Figure 2. Attempts to prepare the analogous six-coordinate Fe(II) complexes, using Fe(II) salts and inert atmospheric conditions, yielded only the Fe(III) species. Furthermore, electrochemical measurements on the [Fe(X-Sal$_2$trien)]$^+$ complexes (see Experimental Section for conditions) also demonstrate a strong preference for the Fe(III) oxidation state with irreversible Fe(III) → Fe(II) reduction waves (DME) for the series occurring at large negative potentials (−1.5 to −2.0 V (SCE)). In the solid state, the room temperature magnetic moments for the parent [Fe(Sal$_2$trien)]$^+$ series are anion and hydration number dependent, spanning the range expected for high-spin Fe(III) with a ^{6}A (O$_h$) ground state (5.81 μ$_B$, anhydrous PF$_6^-$ salt) to low-spin with a ^{2}T (O$_h$) ground state (1.94 μ$_B$, Cl$^-$·2H$_2$O salt). It should be noted that a moment as low as 1.94

μ_B must be considered unusual for low-spin Fe(III) complexes since ^2T ground states usually possess a sizeable orbital contribution to the $S = \frac{1}{2}$ spin-only moment of 1.73 μ_B,[24] e.g., $K_3[Fe(CN)_6]$, μ_{eff} (300 K) = 2.40 μ_B,[25] and $[Fe(phen)_3]$- $(ClO_4)_3$, μ_{eff} (300 K) = 2.45 μ_B.[26] The lowering of the moment toward a spin-only value for a low-spin $[Fe(X-Sal_2trien)]^+$ species can be attributed to effective quenching of the orbital contribution due to a tetragonal distortion which must exist for the molecule. In a tetragonal distorted ligand field, the degeneracy of the octahedral ^2T state would be lifted, $^2T \rightarrow$ $^2E + ^2A$, producing either a ^2E or ^2A state as the actual electronic ground state. Detailed structural information is not yet available for any of the Fe(III) species, but in the case of the $[Ni(Sal_2trien)]$ complex,[21] the degree of this molecular distortion is characterized by Ni–N(amine), Ni–N(imine), and Ni–O bond distances of 2.16, 2.03, and 2.06 Å, respectively.

As solids, all the other $[Fe(X-Sal_2trien)](Y)$ complexes in Table I also exhibit single temperature magnetic moments which fall within and span the entire 1.9–6.0 μ_B range. Assuming magnetically dilute Fe(III) centers in the solid state, the most plausible explanation for such varied magnetic behavior within a structurally similar series involves the postulation of a temperature dependent ^2T (or ^2E, ^2A) $\rightleftarrows$ ^6A spin equilibrium process, with the compounds exhibiting intermediate moments, between the 1.9 (ls) and 6.0 (hs) μ_B limits, being those with the spin crossover region around room temperature. Available solid state variable temperature magnetic susceptibility data for the $[Fe(Sal_2trien)](PF_6)$ compound supports this view with the nearly high-spin room temperature moment of 5.81 μ_B decreasing to 3.86μ_B by 83 K as the result of a rather abrupt change in the μ_{eff} vs. temperature curve at ~200 K (see Experimental Section for data). For spin equilibrium processes, such sharp discontinuities in moment-temperature curves usually result from crystalline phase changes, making theoretical interpretation of solid state magnetic data tenuous at best. In addition, variable temperature Mossbauer spectroscopy, as discussed below for the parent $[Fe(Sal_2trien)](PF_6)$ compound, has been used to further characterize the anomalous magnetic behavior as arising from a $^2T \rightleftarrows ^6A$ spin equilibrium process in the solid state. In this regard, it is interesting to note that these complexes, with their N_4O_2 donor atom set, are the first synthetic Fe(III) $^2T \rightleftarrows ^6A$ spin equilibrium species found to be completely devoid of Fe–S bonding.[44]

The room temperature μ_{eff} value of 2.33 μ_B (295 K) for the $I^-\cdot H_2O$ complex in Table I is somewhat higher than the 1.81 (300 K) value as reported by Sarma and Bailar for their $I^-\cdot$ $1.5H_2O$ salt[22], indicating that the degree of hydration may be an important factor in determining the equilibrium position of the $^2T \rightleftarrows ^6A$ process. In fact, it can be seen from Table I that higher degrees of hydration tend to produce a larger population of the low-spin isomer. This is particularly evident for the $[Fe(Sal_2trien)](Y)$ parent series with the *anhydrous* PF_6^- and BPh_4^- salts having solid state moments in excess of 5.00 μ_B, the *mono-* and *1.5*-hydrate I^- and NO_3^- salts in the range ~2.4 μ_B and the *di*hydrate Cl^- salt having a moment of 1.94 μ_B . Anion and hydration effects on spin equilibria in the solid state have been reported previously,[26] and it is likely that in the present case both effects are operative and nonmutually exclusive. Single-crystal x-ray structural studies now in progress[27] on several $[Fe(X-Sal_2trien)](Y)$ complexes (both hydrated and anhydrous forms) should help clarify the role of the anion/water effect in determining the Fe(III) spin state. More importantly, however, these studies should provide some of the first detailed information describing primary coordination sphere reorganizational processes, e.g., changing Fe–(donor atom) bond distances that accompany changes in the Fe(III) electronic ground state.[39]

To further characterize the new $[Fe(X-Sal_2trien)](Y)$

Table II. Solid State Infrared Data for the $[Fe(Sal_2trien)](Y)$ Complexes as Nujol Mulls at Room Temperature[a,b]

Y	μ_{eff} at 295 K (μ_B)	Lattice H_2O	N—H (st)	C=N (st)	Anion
PF_6^-	5.81		3310 (w)	1618 (s)	835 (s)
				1632 (s)	550 (m)
BPh_4^-	5.08		3245 (w)	1622 (s)	710 (s)[c]
			3220 (w)		850 (w)
					1428 (sh, w)
					1580 (sh, w)
NO_3^- $1.5H_2O$	2.47	3600 (w)	3370 (w)	1635 (s)	d
			3170 (w)		
$I^-\cdot H_2O$	2.33	3600 (w)	3380 (w)	1628 (s)	
			3350 (w)		
			3170 (w)		
			3080 (w)		
$Cl^-\cdot 2H_2O$	1.94	3610 (w)	3480 (w)	1625 (s)	
			3415 (w)		
			3330 (w)		
			3175 (w)		
			3110 (w)		

[a] Band positions in cm^{-1}; estimated error ±3 cm^{-1}. [b] Key: s = strong; m = medium; w = weak intensity relative to base peak; sh = shoulder. [c] Assignments made by analogy with $NaBPh_4$ spectrum. [d] The 1300–1400 cm^{-1} region broadened relative to PF_6^- salt spectrum but no unambiguous NO_3^- absorptions are resolved as reported, for example, for $NaNO_3$ at ~830 and ~1400 cm^{-1}.

complexes, infrared spectra in the 4000–600 cm^{-1} range have been obtained as Nujol mulls. In general, the spectra all display similar features having spectral absorptions attributable to ligand N—H and C=N stretchings, waters of hydration (where applicable), and characteristic anion modes. Assignments for the $[Fe(Sal_2trien)](Y)$ series of compounds, as given in Table II, serve as typical examples for the other $[Fe(X-Sal_2trien)](Y)$ complexes as well and closely follow those reported by Sarma and Bailar for their "low-spin" $[Fe-(Sal_2trien)]I\cdot 1.5H_2O$ salt.[22] Since the Fe(III) spin state for the $[Fe(Sal_2trien)](Y)$ complexes is strongly anion dependent, ranging from nearly high to low spin at room temperature, the spectra have been examined for features which might be diagnostic of the changing spin state. In the 2000–600 cm^{-1} region, no significant anion dependency in the spectra is obvious except, of course, for the characteristic anion modes expected for the differing PF_6^-, BPh_4^-, and NO_3^- counterions. In particular, the absorption assigned to the C=N stretch was of interest since the spin equilibrium Fe(II) complexes, $[Fe(phen)_2(NCS)_2]$[28] and $[Fe(6-MePy_3tren)]^{2+}$ (Figure 1),[29] are each known to exhibit two C—N stretching frequencies corresponding to the high- and low-spin magnetic isomeric forms with $\Delta\nu(C—N) \leq 50$ cm^{-1}. The $[Fe(Sal_2trien)]^+$ complexes show no such obvious C=N(st) multiplicity, with the C=N absorption being an unambiguous doublet only in the case of the nearly high-spin PF_6^- salt. Since variable anion crystal packing effects (in the absence of spin state changes) are also known to produce multiplicity in C=N(st) bands,[30] little significance can be attached to the doubling observed in the case of the PF_6^- salt. It is clear, however, that any differences in the 2000–600 cm^{-1} region of the ir spectrum due to differing Fe(III) spin states are subtle and will require extensive variable temperature/pressure studies for absolute assignment.

As seen from Figure 3, the 3700–3000 cm^{-1} region of the ir spectrum for the $[Fe(Sal_2trien)](Y)\cdot nH_2O$ complexes appear more sensitive to the particular counterion and, therefore,

Table III. Variable Temperature Mossbauer Parameters for the [Fe(Sal₂trien)](PF₆) Complex

$\mu_{eff}.\mu_B$ (K)[a]	δ (mm s⁻¹)[b,c]	ΔE_Q (mm s⁻¹)[d]
5.81 (298)	0.55 (hs singlet)	
5.65 (195)	0.60 (hs singlet)	
4.14 (113)	0.64 (hs singlet)	
	0.49 (ls doublet)	2.97
<3.86 (77)	0.50 (ls doublet)	2.97

[a] Solid state magnetic data taken from experimental section. [b] Relative to 298 K sodium nitroprusside standard. [c] Maximum estimated error: 0.06 mm s⁻¹ (hs peak); 0.02 mm s⁻¹ (ls peak). [d] Maximum estimated error: 0.03 mm s⁻¹.

to the Fe(III) spin state as well. Although not shown in the figure, the spectrum for the $NO_3^-\cdot 1.5H_2O$ salt is similar to that of the $I^-\cdot H_2O$ compound. Room temperature magnetic moment data are set out in Table II along with the ir band assignments. From the table and figure, it is clear that an increase in the low-spin isomer form ($Cl^-\cdot 2H_2O > I^-\cdot H_2O \simeq NO_3^-\cdot 1.5H_2O > BPh_4^- > PF_6^-$) is roughly paralleled by an increase in multiplicity in the spectrum. Definitive band assignments are difficult to make, but, tentatively, the single sharp bands at ~3600 cm⁻¹ for the *hydrated* NO_3^-, I^-, and Cl^- salts have been assigned to lattice water and the multiple pattern of lower energy bands to N-H(st) vibrations. The observed N-H(st) multiplicity probably arises from varying lattice or hydrogen bonding (anion and/or water) environments for N-H functional groups in molecules of the same or even, perhaps, of differing spin. It is unlikely, however, that all the observed multiplicity should be attributed to differing spin state considerations since the $Cl^-\cdot 2H_2O$ salt shows the maximum multiplicity while being essentially only low spin. Whatever the mechanism producing the multiplicity, the ir spectrum in this region can qualitatively be taken as diagnostic of the Fe(III) spin state while serving as a good indication of compound purity as well.

Variable temperature Mossbauer data for the parent PF_6^- compound are presented in Table III. As shown in the table, the spectrum of the fully high-spin form ($T \gtrsim 200$ K) is characterized by a broad singlet (whh $\simeq$ 2 mm s⁻¹) with $\delta \sim$ 0.55 mm s⁻¹ and that of the low-spin form ($T \ll 200$ K) by a quadrupole split doublet (whh $\simeq$ 0.6 mm s⁻¹ for each peak) with $\delta = 0.50$ mm s⁻¹. As the temperature is lowered below the 200 K critical temperature (where the magnetic moment begins to drop from the 5.81 μ_B high-spin value), the high-spin broad singlet gradually decreases in intensity while the intensity of the low-spin doublet increases. At 113 K, with μ_{eff} = 4.14 μ_B (45% hs, 55% ls), peaks for *both* spin states are present, and there is no evidence for an "averaging" of the high- and low-spin peak positions. By 77 K, only the low-spin doublet is unambiguously present; however, the high-spin peak again reappears if the temperature is increasased to 113 K. This pattern is consistent with the presence of an Fe(III) $^2T \rightleftarrows {}^6A$ spin equilibrium and establishes a lower limit of ~10⁻⁷ for the spin state lifetimes, $\tau(^2T)$ and $\tau(^6A)$, in the *solid* state, assuming a dynamic solid state process. Thus, these Fe(III) spin equilibria resemble those reported for cytochrome $P_{450 \text{ camphor}}$[14] and the tris(monothio-β-diketonato)iron(III) complexes[31] which simultaneously show signals for both the low- and high-spin species (τ's > 10⁻⁷ s), but differ from the tris(dithiocarbamato)iron(III) complexes[32] which reportedly show "averaged" spectra (τ's < 10⁻⁷ s). This result for the [Fe(Sal₂trien)](PF₆) complex is especially interesting since, in *solution* near room temperature, $\tau(^2T)$ and $\tau(^6A)$ have been shown, by laser T-jump kinetics, to be $\leq$ 10⁻⁷ s (see spin state lifetime discussion below). Thus, indications are that spin state lifetimes for the [Fe(X-Sal₂trien)]⁺ complexes differ in the
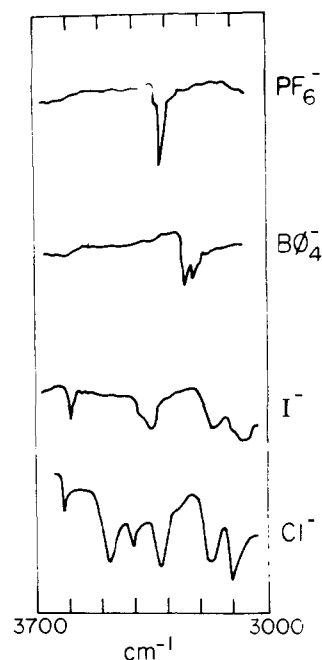

Figure 3. Infrared spectra, as Nujol mulls, in the 3700–3000 cm⁻¹ region for the [Fe(Sal₂trien)](Y)·nH₂O complexes.

solid and *solution* states, e.g., being shorter in solution, especially if the temperature range difference of the two measurements (Mossbauer $\leq$200 K and laser T-jump >273 K) is kept in mind. This conclusion, however, is based on the assumption that a dynamic $^2T \rightleftarrows {}^6A$ spin interconversion occurs in the solid as well as in the solution state. At present there is no evidence to either support or refute a *dynamic* model for these [Fe(X-Sal₂trien)]²⁺ complexes as opposed to a *static* model which assumes the lattice contains a temperature dependent mixture of ^2T and ^6A molecules, perhaps in localized domains. However, variable temperature x-ray photoelectron studies on several tris(dithiocarbamato)iron(III) complexes[45] support the dynamic model for surface lattice molecules in these $^2T \rightleftarrows {}^6A$ complexes, while preliminary studies on the [Fe(6MePy)₃tren](PF₆)₂ $^1A \rightleftarrows {}^5T$ system of Figure 1 are supportive of a static model.[46]

Ligand Substituent Effects on the $^2T \rightleftarrows {}^6A$ Spin Equilibrium in Solution. In contrast to the solid state, single temperature solution magnetic moments in acetonitrile are nearly anion independent for the [Fe(Sal₂trien)](Y) series with all the values falling within the narrow range of 4.94 ($Y^- = I^-$) to 5.16 μ_B ($Y^- = BPh_4^-$) (Table I). This being the case, solution studies seem well suited for the systematic study of ligand substituent and solvent effects on spin equilibria, since unpredictable lattice effects that dominate the Fe(III) spin state in the solid appear to be effectively factored out:

Variable temperature magnetic moment data in acetone for the [Fe(X-Sal₂trien)](PF₆) complexes are shown in Figure 4. Curves for the 3-OCH₃ and 4-OCH₃ derivatives closely resemble that of the 5-OCH₃ compound and have been omitted for purposes of clarity. All data shown in Figure 4 are tabulated in the experimental section. The non-Curie behavior of the μ_{eff} vs. temperature curves is consistent with the presence of an *intra*molecular $^2T \rightleftarrows {}^6A$ equilibrium process since in solution (1) the Fe(III) centers must be considered magnetically dilute, (2) magnetic moment values span the same 1.9–6.0 μ_B range as found for the anion dependent $^2T \rightleftarrows {}^6A$ process in the solid, and (3) the anomalous magnetic behavior is accompanied by rather striking thermochromism of the nature known to accompany other iron spin equilibrium processes.[8] Furthermore, all the curves are characteristically smooth, generally parallel,
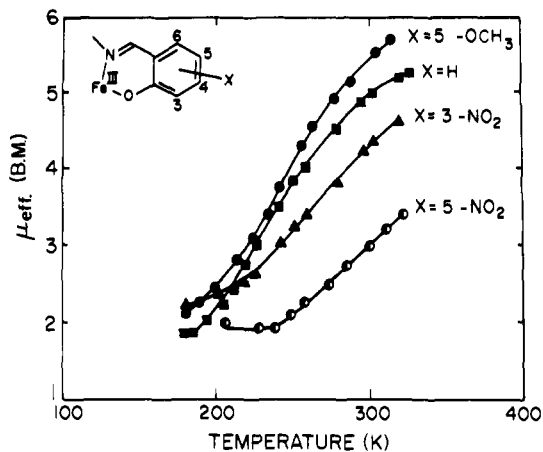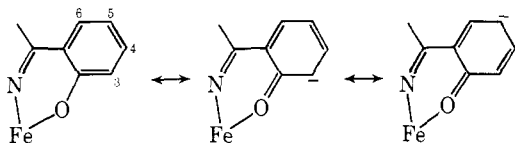
Figure 4, μ_{eff} vs. temperature curves in acetone for the [Fe(X-Sal$_2$-trien)](PF$_6$) complexes.

Table IV. Solvent Dependency of the Solution Magnetic Moment for the [Fe(Sal$_2$trien)](PF$_6$) Complexes

Solvent	μ_{eff} (μ_B) at 307 K[b]	Solvent	μ_{eff} (μ_B) at 307 K[b]
C$_6$H$_5$NO$_2$	5.50	CH$_3$OH	4.81
CH$_2$Cl$_2$	5.41	CH$_3$COCH$_3$–H$_2$O[a]	4.53
CH$_3$NO$_2$	5.28	C$_5$H$_5$N	4.45
CH$_3$COCH$_3$	5.05	DMF	4.36
CH$_3$CN	5.01	HMPA	4.10
CH$_3$COCH$_3$–CH$_3$CN[a]	4.93	Me$_2$SO	4.02

[a] A 50:50 mole fraction measured by weight. [b] Estimated maximum error: 0.10 μ_B.

and noticeably lacking of sharp discontinuities of the type found for the [Fe(Sal$_2$trien)](PF$_6$) compound in the solid state.

Assuming values of 6.0 and 1.9 μ_B as the limiting high- and low-spin moments, the percent of high-spin isomer for the [Fe(X-Sal$_2$trien)](PF$_6$) complexes in acetone at room temperature decreases according to the salicylaldimine ring substituent series: 4-OCH$_3$ (97%) > 5-OCH$_3$ (85%) > 3-OCH$_3$ (73%) > H (68%) > 3-NO$_2$ (49%) > 5-NO$_2$ (19%). Furthermore, the variable temperature studies in Figure 4 confirm this to be the general pattern over a wide temperature range. The nature of this substituent effect must be electronic in origin since the spatial orientation of the two chelated salicylaldimine rings (ref 21 and Figure 2) indicate no obvious *intra*molecular substituent steric interactions of the same nature as responsible for production of the spin equilibrium phenomena in the [Fe(6-MePy)$_n$(Py)$_m$tren]$^{2+}$ series of complexes.[8a] In general, for the [Fe(X-Sal$_2$trien)]$^+$ series the more electronegative NO$_2$ groups favor the low-spin isomer while OCH$_3$ groups produce more of the high-spin form, with the unsubstituted parent compound exhibiting an intermediate behavior. A similar substituent effect has also been noticed by Ho and Livingstone in their solid state studies of substituted tris(monothio-β-diketonato)iron(III) ^{2}T $\rightleftharpoons$ ^{6}A complexes[33] where electronegative CF$_3$ substituents favored the low-spin state relative to CH$_3$ groups.

In addition, for the [Fe(X-Sal$_2$trien)]$^+$ complexes, the substituent position appears to be nearly as important as the substituent kind in influencing the ^{2}T $\rightleftharpoons$ ^{6}A equilibrium. This effect is exemplified most strikingly by comparison of the 3- and 5-NO$_2$ compounds. The fact that the 5-NO$_2$ group is in the most remote position from the metal center, while at the same time causing the largest deviation in magnetic behavior from the parent compound, is strong evidence for the presence of a substituent dependent Fe–ligand (π) bonding interaction. Qualitatively, the following ring π-resonance structures may be written as shown below, which formally place negative

charge on the 3 and 5 positions of the salicylaldimine ring. Electron-withdrawing groups, such as NO$_2$, at these positions would serve to further delocalize this charge, thereby increasing the degree of any Fe $\rightarrow$ ligand (π) bonding. This increased π delocalization (into empty π^* orbitals) could then

result in an increase in the ligand field splitting parameter, Δ, with a concomitant increase in the low-spin isomer population. By analogy, OCH$_3$ groups, which are electron donating in a π-resonance sense, would decrease Δ, resulting in a relative increase in the high-spin isomer population, as is experimentally observed. Judging from the degree of change in the isomer populations as the substituent is varied, Δ can be adjusted by several hundred wavenumbers by the Fe $\rightarrow$ ligand(π) delocalization mechanism. Of course, any complete bonding scheme must also consider substituent σ-inductive effects. However, since both NO$_2$ and och$_3$ groups are electron withdrawing in this sense, σ-inductive considerations alone do not adequately explain the observed opposite effect on the spin equilibrium caused by this pair of substituents. Moreover, if a σ-type mechanism were of predominant importance, NO$_2$ group substitution in the 3 position should have a greater effect, relative to the unsubstituted parent compound, than substitution in the 5 position, and this is not the case. Rather, it appears that the major substituent perturbations here are of Fe$\rightarrow$ligand(π) origin with an overlying, but probably less significant, Fe$\rightarrow$ligand(σ) contribution. Studies are continuing on an expanded series of [Fe(X-Sal$_2$trien)]$^+$ complexes and on other structurally related spin equilibrium species, e.g., [Fe(X-Acac$_2$trien)]$^+$ and [Fe(X-Trop$_2$trien)]$^+$ (where Acac = acetylacetone and Trop = tropolone) to test further the general pattern of these group substituent effects and to ascertain the maximum degree of control over spin equilibria afforded by peripheral ligand substitution. In this regard, the most subtle possible substituent variation for the [Fe(X-Sal$_2$trien)]$^+$ complexes is isotopic in nature, with N–D groups substituted for N–H groups on the trien backbone. However, for the [Fe(Sal$_2$trien-d_2)](PF$_6$) complex in CH$_2$Cl$_2$ (the best solvent for no H–D exchange), variable temperature (180–307 K) magnetic susceptibility data were found to be experimentally indistinguishable from those of the N–H parent compound.

Solvent Effects on the ^{2}T $\rightleftharpoons$ ^{6}A Spin Equilibrium. Early in our studies on the parent [Fe(Sal$_2$trien)]$^+$ complex, we noticed that the color of its room temperature solutions was strikingly solvent dependent. For example, solutions of the PF$_6^-$ salt in CH$_2$Cl$_2$, CH$_3$NO$_2$, and C$_6$H$_5$NO$_2$ were found to be red in color, whereas solutions of DMF, HMPA, and Me$_2$SO were distinctly more purple. Moreover, this pattern of colors appeared essentially counterion independent. The reason for this solvent dependent chromism becomes clear from Table IV where room temperature magnetic moments for the [Fe(Sal$_2$trien)](PF$_6$) complex are reported as a function of solvent and mixed-solvent systems. From these data, it is seen that the magnetic moments are strongly solvent dependent and that those solvents which produce more high-spin character ($\mu_{eff} \geq 5.0$ μ_B) give correspondingly red solutions, whereas those which produce more low-spin character (4.0 $\lesssim \mu_{eff} \lesssim 4.5$ μ_B)

Table V. Thermodynamic Parameters for the [Fe(X-Sal$_2$trien)](PF$_6$) Complexes in Solution

Substituent	Solvent	$\Delta H°$ (kcal mol^{-1})^a	$\Delta S°$ (eu)^a	T (K)^b
H	Acetone	4.62 ± 0.08	16.46 ± 0.50	186–326
	CH$_3$CN	3.76 ± 0.11	13.85 ± 0.81	242–307
	CH$_3$OH	3.75 ± 0.06	12.83 ± 0.41	256–323
	Acetone–H$_2$O^c	5.02 ± 0.13	16.60 ± 0.90	238–309
	C$_5$H$_5$N	4.13 ± 0.17	13.36 ± 1.21	242–307
3-OCH$_3$	Acetone	3.54 ± 0.09	14.57 ± 0.82	202–319
4-OCH$_3$	Acetone	5.28 ± 0.14	21.79 ± 1.10	192–299
5-OCH$_3$	Acetone	4.27 ± 0.09	16.74 ± 0.40	183–314
3-NO$_2$	Acetone	3.81 ± 0.04	12.51 ± 0.32	181–319
5-NO$_2$	Acetone	5.99 ± 0.25	16.33 ± 1.64	239–322

^{a} Thermodynamic parameters (and standard deviations) as calculated from the magnetic susceptibility data given in the experimental section, assuming K = [hs]/[ls] and limiting values of 1.9 (ls) and 6.0 μ_B (hs). ^{b} Temperature interval over which the ln K vs. T^{-1} and $\Delta G°$ vs. T plots appear linear as shown in Figure 6. ^{c} A 50:50 mole fraction measured by weight.
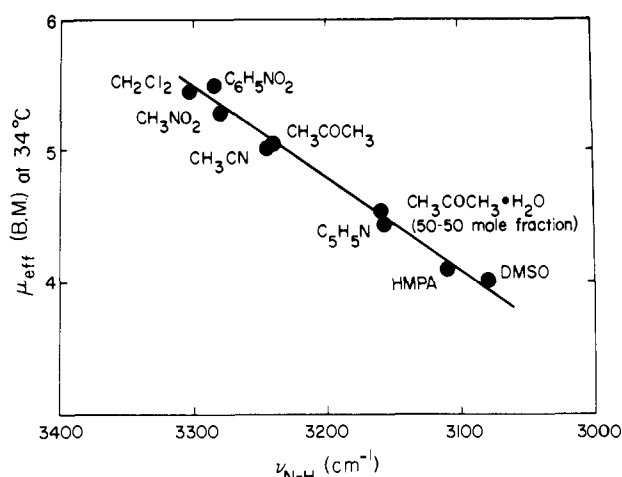
Figure 5. μ_{eff} vs. $\nu_{N-H(st)}$ correlation for the [Fe(Sal$_2$trien)](PF$_6$) complex in various solvents.

Figure 6. A typical ln K vs. T^{-1} and $\Delta G°$ vs. T plot for the [Fe(Sal$_2$-trien)](PF$_6$) complex in acetone.

give the purplish colored solutions. Examination of molecular models revealed that a particularly inviting site for a specific {[Fe(Sal$_2$trien)]$^+$·solvent} interaction might be at the coordinated secondary amine protons of the trien backbone. For this reason, the N–H stretching frequency in the ir for the [Fe-(Sal$_2$trien)](PF$_6$) parent compound was measured in a variety of solvents and correlated to the compound's magnetic behavior in each solvent. The results, as shown in Figure 5, indicate a nearly linear relationship between ν_{N-H} and the measured magnetic moment for a rather diverse series of nitrogen and oxygen containing solvents. The observed shifts of ν_{N-H} to lower energy, with band broadening, is that which would be expected for an [N–H···solvent] hydrogen bonding interaction.[34] Assuming $\nu_{N-H(free)}$ 3300 cm^{-1} in CH$_2$Cl$_2$, $\Delta\nu_{N-H}$ (cm^{-1}) data for the {[Fe(Sal$_2$trien)]$^+$·solvent} series in Figure 5 are: C$_6$H$_5$NO$_2$ (15) < CH$_3$NO$_2$ (20) < CH$_3$CN (55) < acetone (60) < 50–50 acetone–H$_2$O (140) < pyridine (142) < HMPA (190) < Me$_2$SO (220).

Assignment of the observed $\Delta\nu_{N-H}$ shifts to hydrogen bonding is further substantiated by a similar solvent ordering reported in hydrogen bonding studies of pyrrole with various solvent bases.[35] In addition, from calorimetry studies by Drago and Nozari,[36] an energetic relationship for the [pyrrole–solvent] hydrogen bonding interaction, $\Delta\nu_{N-H}$ (cm^{-1})/$-\Delta H$ (kcal mol^{-1}), yields estimates in pyridine of 50 cm^{-1}/kcal mol^{-1}, Me$_2$SO (44), CH$_3$CN (30), and acetone (29). Assuming that a similar $\Delta\nu_{N-H}/-\Delta H$ relationship holds for the {[Fe(Sal$_2$trien)]$^+$·solvent} hydrogen bonding, $-\Delta H$/(Fe complex) $\simeq$ 10 kcal mol^{-1} for Me$_2$SO, 6 (pyridine), 5 (acetone), and 4 (CH$_3$CN). A hydrogen bonding interaction of

such magnitude, involving protons on coordinated nitrogen donor atoms and solvating molecules, would seem capable of increasing Δ sufficiently ($<kT$ or 0.6 kcal mol^{-1}) to increase the low-spin isomer population by as much as 44% in Me$_2$SO relative to "high-spin" (weakly hydrogen bonding) solvents such as CH$_2$Cl$_2$, C$_6$H$_5$NO$_2$, or CH$_3$NO$_2$. While a [metal complex·solvent] hydrogen bonding interaction appears to explain satisfactorily the solvent effect on these [Fe(X-Sal$_2$trien)]$^+$ ^{2}T $\rightleftarrows$ ^{6}A processes, other possible effects in solution such as molecular aggregation by ion pairing or [complex·solvent] charge transfer π-adduct formation must also be considered as potentially important until proven otherwise. Aggregation and foreign substance studies (electrolytes, polypeptides, etc.) are continuing for these and other solution state spin equilibria in attempts to assess the importance of these types of molecular "solvation" interactions.

Solution state thermodynamic parameters for the [Fe(X-Sal$_2$trien)]$^+$ ^{2}T $\rightleftarrows$ ^{6}A processes, as calculated from the magnetic susceptibility data, are shown in Table V. Typical least-squares fitted ln K vs. T^{-1} and $\Delta G°$ vs. T plots used to obtain the $\Delta H°$ and $\Delta S°$ parameters are shown in Figure 6. In general, the $\Delta H°$ and $\Delta S°$ values are all very similar, regardless of the substitution kind, its position, or the solvent system. Qualitatively, the major contribution to the observed $\Delta H°$'s probably reflects the changing Fe–(donor atom) bond distances and energies that are known to accompany spin conversion processes. The $\Delta H°$ values in Table V for these Fe(III) ^{2}T $\rightleftarrows$ ^{6}A processes compare favorably to those reported for the two Fe(II) ^{1}A $\rightleftarrows$ ^{5}T spin equilibria that have also been studied in solution: [Fe(6-MePy)$_2$(Py)tren]$^{2+}$ ($\Delta H°$ = 4.6 kcal mol^{-1})[8a] and bis(hydrotrispyrazolylborate)iron(II) ($H°$ = 3.9 kcal mol^{-1}).[7] No x-ray structural information is yet available for any [Fe(X-Sal$_2$trien)]$^+$ species, but for the Fe(II) ^{1}A $\rightleftarrows$ ^{5}T processes, variable temperature structural data for [Fe-
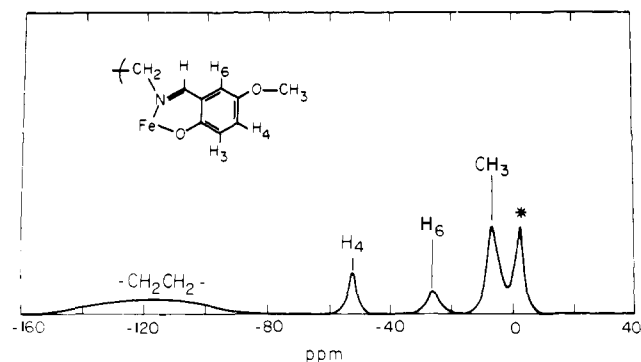
Figure 7. Proton magnetic resonance spectrum of the [Fe(5-OCH₃-Sal₂trien)](PF₆) complex in acetone-d_6 at 307 K, with the solvent peak (*).

Table VI. Proton Magnetic Resonance Data for the [Fe(X-Sal₂trien)]⁺ Complexes as PF₆⁻ Salts in Acetone-d_6 at ~34 °C[a]

X	-CH₂CH₂-	H₄	H₆	-OCH₃	Solvent (*)
H	−111	−30	−11		+20
3-OCH₃	−137	−57	−28	0	+6
4-OCH₃	−149		−16	+9	+11
5-OCH₃	−130	−46	−29	−6	+2
3-NO₂	b	−44	−28		0

[a] Peak positions reported relative to external Me₄Si in ppm; estimated error for H₄, H₆, and OCH₃, 2 ppm, and for -CH₂CH₂-, 5 ppm. [b] Too broad for accurate peak position assignment.

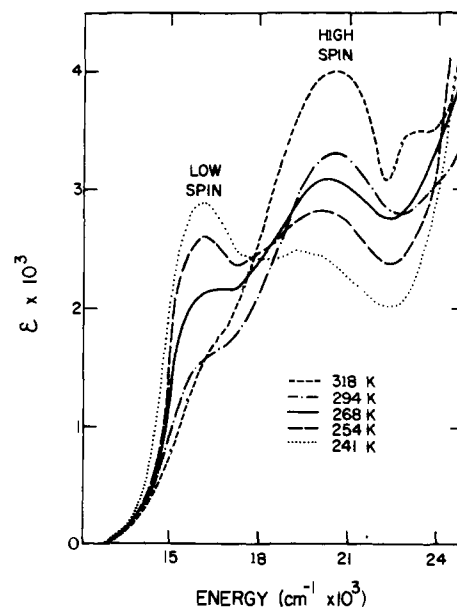(bpy)₂(NCS)₂][37] and [Fe(6-MePy)₃tren]²⁺ [38] reveal that the average Fe–N bond distances decrease by ≥0.12 Å upon the $^5T \rightarrow {}^1A$ spin conversion. Judging from the similarities in $\Delta H°$ values for all these iron spin equilibria, it seems likely that the $^6A \rightarrow {}^2T$ spin conversions for the [Fe(X-Sal₂trien)]⁺ complexes will result in primary coordinate sphere reorganization of comparable magnitude. In comparison, for the tris(N,N-R₂dithiocarbamato)iron(III) complex (R = Et) the average Fe–S bond distance decreased by only ~0.05 Å[39] upon a partial $^6A \rightarrow {}^2T$ spin conversion, with the accompanying $\Delta H°$ value of ~2 kcal mol⁻¹ in acetone (unpublished results for the R = Me derivative) being appreciably smaller. The $\Delta S°$ values reported in Table V partially reflect the "electronic entropy change" of $R \ln {}^6/_6$ or 0 eu expected for these $^2T \rightleftarrows {}^6A$ processes, with the remaining $\Delta S°$ contribution likely arising from solvation sphere reorganization accompanying spin conversion. Thus, a small solvent and substituent dependency on $\Delta S°$, as observed, is not unexpected. However, the $\Delta S°$ values of these [Fe(X-Sal₂trien)]⁺ $^2T \rightleftarrows {}^6A$ processes are noticeably larger than the 8–12 eu[7,8a] range reported for the two Fe(II) spin equilibrium compounds in solution.

Spin State Lifetime Considerations. As discussed above, Mossbauer spectroscopy has demonstrated for the [Fe(Sal₂trien)](PF₆) complex with a dynamic $^2T \rightleftarrows {}^6A$ process that the spin state lifetimes, $\tau(^2T)$ and $\tau(^6A)$, in the solid at ≤200 K, are ≳10⁻⁷ s. In order to obtain comparative estimates for spin lifetimes in *solution*, several of the [Fe(X-Sal₂trien)]⁺ derivatives have been studied by variable temperature uv-visible and ¹H NMR spectroscopy. In addition, estimates obtained by these techniques have been further refined by the direct measurement of τ using the laser Raman temperature-jump technique.

The ¹H NMR spectrum of the X = 5-OCH₃ derivative in acetone-d_6 at 34 °C (μ_{eff} = 5.50 μ_B; 85% hs) is shown in Figure 7. The assignments, as shown in the figure, for this compound and for the other derivatives in Table VI have been made by X-group substitution and by consideration of the fact that the methylene and H₆ resonances are common to all the spectra. In no case was a signal found in any of the spectra that could be assigned to an H₃ proton, and presumably, this resonance is too far shifted and/or broadened by the close proximity of the proton to the paramagnetic Fe(III) center to be resolved from the spectrum baseline.

At room temperature, the 5-OCH₃ spectrum is essentially that of a ^6A high-spin Fe(III) complex and, as such, the observed resonance positions are mainly of Fermi contact origin. As the temperature is lowered, all the signals broaden but with seemingly little change in their absolute positions. By −30 °C (μ_{eff} = 3.75 μ_B; 33% hs) the methylene signal disappears due to broadening, and by −50 °C (μ_{eff} = 3.10 μ_B; ~19% hs) only the methyl (−4 ppm) and solvent peaks (+2 ppm) are still

Figure 8. Variable temperature electronic spectrum of the [Fe-(Sal₂trien)](PF₆) complex in acetone at ~10⁻⁴ M.

discernible. This pattern is reconcilable in terms of the expected non-Curie behavior accompanying the $^2T \rightleftarrows {}^6A$ spin equilibrium in which the low-spin ^2T state population is steadily increased. The observed peak broadening with decreasing temperature (even though the magnetic susceptibility also decreases) is attributed to a shorter and, therefore, more unfavorable, spin-lattice relaxation time associated with the ^2T state.[40] While the ^2T state is expected to produce a large dipolar shift contribution to the observed spectrum, as in the case of the low-spin [Fe(bpy)₃]³⁺ cation,[41] severe spectral broadening for these ^2T state [Fe(X-Sal₂trien)]⁺ complexes precludes any meaningful factoring of isotropic shifts into their contact and dipolar components.

The ¹H NMR data for the [Fe(X-Sal₂trien)]⁺ series of complexes appear to be consistent with a rapid $^2T \rightleftarrows {}^6A$ spin equilibrium, giving rise to a mole-fraction-weighted average resonance position. Assuming that exchange is in the fast exchange temperature region, the appropriate expression for the spin state lifetime, τ, is $\tau \ll 1/[2\pi(\delta\omega)]$ where $\delta\omega$ is the frequency separation, in hertz, between the two exchanging magnetic isomers in the absence of exchange. Thus, assuming shifts as large as 150 ppm at 60 MHz for the ^6A (hs) state, as is observed for the [Fe(4-OCH₃Sal₂trien)]⁺ species at 310 K (μ_{eff} = 5.91 μ_B), and shifts of approximately 50 ppm[41] as found for the ^2T (ls) complex, [Fe(bpy)₃]³⁺, the upper limit for τ is 3×10^{-4} s.

The variable temperature electronic spectrum of [Fe(Sal₂trien)](PF₆) dissolved in acetone is shown in Figure 8. In general, the spectrum is characterized in the visible by a low

Table VII. Electronic Spectral Data for the [Fe(X-Sal$_2$trien)]-(PF$_6$) Complexes in Acetone^a at Room Temperature

Substituent	$\nu_{(max)}$, cm^{-1}	$\epsilon_{(max)}{}^b$
Parent	16 130 (ls)	1 900
	20 410 (hs)	3 600
	23 260	3 000
	29 410	9 700
3-OCH$_3$	18 870	3 800
	28 570	9 700
4-OCH$_3$	20 200 (hs)	3 500
	26 320	6 000
	29,410	9 000
5-OCH$_3$	18 180 (hs)	3 900
	20 410	3 800
	27 780	9 700
3-NO$_2$	16 950 (ls)	1 000
	20 830 (hs)	1 800
	27 400	7 000
5-NO$_2$	16 950 (ls)	2 500
	19 230 (hs)	2 000
	27 030	>10 000

^{a} Approximately 10^{-4} M. ^{b} Determined at $\nu_{(max)}$ without deconvolution.

energy CT band centered at ~16 000 cm^{-1} (ϵ ~2000) which increases in intensity with decreasing temperature (the LOW-SPIN band) and a higher energy band at ~20 000 cm^{-1} (ϵ ~ 3600) which decreases in intensity with decreasing temperature (the HIGH-SPIN band). A careful search on the low energy side of these bands revealed no low intensity bands of purely d–d character. The strong temperature dependency of the [Fe(Sal$_2$trien)]$^+$ spectrum is typical of the entire series of complexes and explains their striking thermochromic behavior in solution. Typical thermochromism for each compound is documented in the experimental section, and room temperature spectral parameters characterizing the PF$_6{}^-$ salts in acetone are given in Table VII, along with their respective (hs) and (ls) band assignments. The presence of distinct (hs) and (ls) bands, whose relative intensities vary with temperature, is consistent with a ^{2}T $\rightleftarrows$ ^{6}A spin interconversion process which is slow on the ~10^{-15} s electronic transition time scale.

Together, the ^{1}H NMR and electronic spectral data establish the working limit for these Fe(III) spin lifetimes in solution as 10^{-15} s $< \tau < 10^{-4}$ s. Recently, we have further refined these estimates by using the laser Raman temperature-jump technique to measure $\tau(^2$T) and $\tau(^6$A) directly for the [Fe(Sal$_2$trien)]$^+$ parent compound in methanol. This same technique has also been employed by Beattie et al.[42] and ourselves[43] to measure spin lifetimes for the Fe(II) ^{1}A $\rightleftarrows$ ^{5}T (or ^{5}A) spin equilibrium compounds [Fe(pyrazolylborate)$_2$] ($\tau(^1$A) = 1 × 10^{-7}, $\tau(^5$A) = 5 × 10^{-8} s) at 20°C in CH$_2$Cl$_2$/MeOH and [Fe(6-MePy)$_2$(Py)tren]$^{2+}$ of Figure 1 ($\tau(^1$A) = 2.5 × 10^{-7}, $\tau(^5$A) = 2.0 × 10^{-7} s) at 21°C in acetone (10%)–MeOH. The corresponding $\tau(^2$T) and $\tau(^6$A) values for [Fe(Sal$_2$trien)](PF$_6$) in methanol are $\tau(^2$T) = 7.1 × 10^{-8} and $\tau(^6$A) = 6.7 × 10^{-8} s at 20°C and $\tau(^2$T) = 1.2 × 10^{-7} and $\tau(^6$A) = 1.1 × 10^{-7} s at 4°C. Thus, available results indicate that dynamic spin state lifetimes in solution for these Fe(III) spin equilibria (1) are similar to those found for the Fe(II) processes, (2) approach the Mossbauer (solid state) observation time scale, and (3) are unlikely to be rate determining for most, if not all, outer-sphere electron transfer reactions that the compounds may undergo.

References and Notes

(1) Presented in part at the Southwest Regional Meeting of the American Chemical Society, Houston, Texas, Dec 1974, and the combined Southwest-Southeast Regional Meeting of the American Chemical Society, Memphis, Tenn., Oct 1975.
(2) Robert A. Welch Foundation Graduate Fellow.
(3) L. Cambi and A. Cagnosso, *Atti Accad. Naz. Lincei*, **13**, 809 (1931); L. Cambi and L. Szego, *Ber.*, **64**, 2591 (1931); L. Cambi, L. Szego, and A. Cagnasso, *Atti Accad. Naz. Lincei.*, **15**, 266, 329 (1932); L. Cambi and L. Szego, *Ber.*, **66**, 656 (1933).
(4) R. L. Martin and A. H. White, *Transition Met. Chem.*, **4**, 113 (1968); E. K. Barefield, D. H. Busch, and S. M. Nelson, *Q. Rev., Chem. Soc.*, **22**, 457 (1968).
(5) R. M. Golding, W. C. Tennant, C. R. Kanekar, R. L. Martin, and A. H. White, *J. Chem. Phys.*, **45**, 2688 (1966).
(6) L. H. Pignolet, G. S. Patterson, J. F. Weiher, and R. H. Holm, *Inorg. Chem.*, **13**, 1263 (1974).
(7) J. P. Jesson, S. Trofimenko, and D. R. Eaton, *J. Am. Chem. Soc.*, **89**, 3158 (1967).
(8) (a) M. A. Hoselton, L. J. Wilson, and R. S. Drago, *J. Am. Chem. Soc.*, **97**, 1722 (1975); (b) L. J. Wilson, D. Georges, and M. A. Hoselton, *Inorg. Chem.*, **14**, 2968 (1975).
(9) J. K. Beattie, N. Sutin, D. H. Turner, and G. W. Flynn, *J. Am. Chem. Soc.*, **95**, 2052 (1973).
(10) H. Taube, "Electron Transfer Reactions of Complex Ions in Solution", Academic Press, New York, N.Y. 1970; M. C. Palazzotto and L. H. Pignolet, *Inorg. Chem.*, **13**, 1781 (1974).
(11) R. Chant, A. R. Hendrickson, R. L. Martin, and N. M. Rohde, *Inorg. Chem.*, **14**, 1894 (1975).
(12) F. Basolo and R. G. Pearson, "Mechanisms of Inorganic Reaction", Wiley, New York, N.Y., p 512.
(13) D. F. Wilson, P. L. Dulton, M. Erecinsha, J. G. Lindsay, and N. Sato, *Acc. Chem. Res.*, **5**, 234 (1972); I. Morishima and T. Jizaka, *J. Am. Chem. Soc.*, **96**, 5279 (1974).
(14) M. Sharrock, E. Munck, P. G. Debrunner, V. Marshall, J. D. Lipscomb, I. C. Gunsalus, *Biochemistry*, **12**, 258 (1973).
(15) D. H. Turner, G. W. Flynn, N. Sutin, and J. V. Beitz, *J. Am. Chem. Soc.*, **94**, 1554 (1972).
(16) D. F. Evans, *J. Chem. Soc.*, 2003 (1959).
(17) D. Ostfeld and I. A. Cohen, *J. Chem. Educ.*, **49**, 829 (1972).
(18) K. Weigehausen, M. L. Rudee, and R. B. McLellan, *Acta Metall.*, **21**, 589 (1973).
(19) B. L. Chrisman and T. A. Tumolillo, *Comput. Phys. Commun.*, **2**, 322 (1971).
(20) A. K. Mukherjee, *Sci. Cult.*, **19**, 107 (1953).
(21) P. D. Cradwick, M. E. Cradwick, G. G. Dodson, D. Hall, and T. N. Waters, *Acta Crystallogr., Sect. B*, **28**, 45 (1972).
(22) B. D. Sarma and J. C. Bailar, Jr., *J. Am. Chem. Soc.*, **77**, 5476 (1955).
(23) K. Kunze, M. Tweedle, and L. J. Wilson, to be submitted for publication; D. Cullen and L. J. Wilson, to be submitted for publication.
(24) B. N. Figgis, *Trans. Faraday Soc.*, **57**, 204 (1961).
(25) J. B. Howard, *J. Chem. Phys.*, **3**, 813 (1935).
(26) R. N. Sylva and H. A. Goodwin, *Aust. J. Chem.*, **20**, 479 (1967).
(27) D. Cullen and L. J. Wilson, to be submitted for publication.
(28) E. Konig and K. Madeja, *Spectrochim. Acta, Part A*, **23**, 45 (1967).
(29) L. J. Wilson, E. V. Dose, M. G. Simmons, and M. Tweedle, Abstracts of the 169th National Meeting of the American Chemical Society, Philadelphia, Pa., April 1975, INOR 168.
(30) L. J. Wilson, Ph.D. Dissertation, University of Washington, Seattle, Wash., 1971.
(31) M. Cox, J. Darken, B. W. Fitzsimmons, A. W. Smith, L. F. Larkworthy, and K. A. Rogers, *J. Chem. Soc., Dalton Trans.*, 1192 (1972).
(32) R. Rickards, C. E. Johnson, and H. A. O. Hill, *J. Chem. Phys.*, **48**, 5231 (1968).
(33) R. K. Y. Ho and S. E. Livingstone, *J. Aust. Chem.*, **21**, 1987 (1968).
(34) K. Nakanishi, "Infrared Absorption Spectroscopy", Nankodo, 1964, p 38.
(35) L. J. Bellamy, H. E. Hallam, and R. L. Williams, *Trans. Faraday Soc.*, **54**, 1120 (1958); F. Strohbush and H. Zimmerman, *Ber. Bunsenges. Phys. Chem.*, **71**, 567 (1967); M. L. Joslen an N. Fuson, *J. Chem. Phys.*, **22**, 1169, 1264 (1954).
(36) M. S. Nozari and R. S. Drago, *J. Am. Chem. Soc.*, **92**, 7086 (1970).
(37) E. Konig and K. J. Watson, *Chem. Phys. Lett.*, **6**, 457 (1970).
(38) Reference 8a.
(39) J. G. Leipoldt and P. Coppens, *Inorg. Chem.*, **12**, 2269 (1973).
(40) R. S. Drago, "Physical Method in Inorganic Chemistry", Reinhold, New York, N.Y. 1975, p 298.
(41) R. E. DeSimone and R. S. Drago, *J. Am. Chem. Soc.*, **92**, 2343 (1970).
(42) Reference 9.
(43) M. H. Hoselton, R. S. Drago, N. Sutin, and L. J. Wilson, Abstracts of the Southwest Regional Meeting of the American Chemical Society, Houston, Texas, Dec 1974; ref 29; M. H. Hoselton, R. S. Drago, N. Sutin, and L. J. Wilson, *J. Am. Chem. Soc.*, in press.

(44) Several heme proteins such as metmyoglobin hydroxide and methemo-globin hydroxide (and other derivatives) contain spin equilibrium Fe(III), but it is not certain whether or not a change in coordination number from six to five is also involved. See for example: J. K. Beattie and R. J. West, *J. Am. Chem. Soc.*, **96**, 1933 (1974). In this work, the high-spin and low-spin "states" of a metmyoglobin hydroxide are reported to have spin lifetimes of <5 μs.

(45) M. J. Tricker, *J. Nucl. Chem.*, **36**, 1543 (1974).

(46) E. V. Dose, M. F. Tweedle, L. J. Wilson, and C. Wagner, to be submitted for publication.

Coordination Properties of o-Benzoquinones. Structure and Bonding in Tris(tetrachloro-1,2-benzoquinone)chromium(0)

Cortlandt G. Pierpont*[1] and Hartley H. Downs

Contribution from the Department of Chemistry, West Virginia University, Morgantown, West Virginia 26506. Received August 28, 1975

Abstract: Addition of tetrachloro-1,2-benzoquinone to $Cr(CO)_6$ leads to formation of tris(tetrachloro-1,2-benzoquinone)chromium. Crystals of the complex prepared in benzene and recrystallized from CS_2 are isolated as the mixed solvate $Cr(O_2C_6Cl_4)_3 \cdot CS_2 \cdot \frac{1}{2}C_6H_6$. They crystallize in a triclinic cell, space group $P\bar{1}$ with $a = 7.904$ (3) Å, $b = 16.192$ (4) Å, $c = 13.848$ (4) Å, $\alpha = 101.27$ (4)°, $\beta = 82.78$ (4)°, and $\gamma = 126.68$ (4)°. There are two formula weights per unit cell. The structure was solved by conventional Patterson, Fourier, and least-squares procedures using x-ray data complete to $2\theta = 50°$ (Mo Kα radiation). Refinement of the structure converged with final discrepancy indices of $R = 0.045$ and $R_w = 0.044$ for 2237 observed reflections. The coordination geometry of $Cr(O_2C_6Cl_4)_3$ is octahedral. Structural features of the ligands indicate that they remain unreduced on coordination, bonding to the Cr(0) metal center as benzoquinones. The cationic Cr(I) complex $Cr(O_2C_6Cl_4)_3{}^+$ exhibits an ESR spectrum with an unusually low g value of 1.969 (1) and strong ^{53}Cr coupling of 27.5 (5) G. The properties of these complexes suggest a highly localized electronic structure with little contribution from quinone π* levels.

The 1,2-benzoquinones appear to be an unusually diverse series of ligands. Investigations carried out on molybdenum-quinone complexes have provided examples where the ligands bond in various electronic forms, formally as catecholates, semiquinone radical-anions, or as unreduced benzoquinones. While charge delocalization over the chelate ring is possible, similar to the related 1,2-dithiolene ligands, specific structural features have provided information regarding metal and ligand oxidation states. In the coordination chemistry of molybdenum, cis-dioxo ligands are characteristic of Mo(VI). Thus 9,10-phenanthrenequinone ligands in $Mo_2O_5(O_2C_{14}H_8)_2{}^2$ and $MoO_2Cl_2(O_2C_{14}H_8)^3$ bond as semiquinone and benzoquinone ligands, respectively. Bridging tetrachloro-1,2-benzoquinone ligands in $[Mo(O_2C_6Cl_4)_3]_2$ possess features consistent with catecholate coordination.[4] The electronic diversity of the molybdenum–quinone system relates to the natural selection of Mo in specific biological electron transfer systems involving the quinoid flavins.[5]

Synthetically, complexes of 1,2-benzoquinones may be formed by addition of the ligand to a complex containing the desired metal in a low oxidation state. Oxidative addition reactions have been used to synthesize catecholate adducts of group 8 metal systems.[6] Others have examined the direct reaction of quinones with metal carbonyls as a means of preparing binary quinone complexes.[7] We have reported the addition of tetrachloro-1,2-benzoquinone to the carbonyls of group 6a metals yielding tris complexes (eq 1).[8] The Mo and

W complexes of this series have been found to be dimeric with bridging and chelating quinone ligands.[4] The geometries are octahedral, and ligand reduction occurs on coordination. The Cr complex is considerably different. From spectral and electrochemical data the complex appears monomeric, undergoing three reversible oxidation reactions to complexes with charges of +1, +2, and +3. Recent results obtained from the addition of tetrachlorocatecholate to Cr(III) salts suggest an analogous series of anionic compounds, as well.[9] In view of the unusual molecular geometry of $[Mo(O_2C_6Cl_4)_3]_2$, the apparent differences between this complex and its Cr analogue, and the trigonal prismatic structure of the 9,10-phenan-threnequinone complex $Mo(O_2C_{14}H_8)_3$,[10] we have undertaken a crystallographic molecular structure determination on $Cr(O_2C_6Cl_4)_3$. We wish to report the results of that investigation with some pertinent paramagnetic resonance data on the related cationic complex $Cr(O_2C_6Cl_4)_3{}^+$ generated synthetically.

Experimental Section

Preparation of $Cr(O_2C_6Cl_4)_3$. The complex was prepared by refluxing 6.1 g of tetrachloro-1,2-benzoquinone (25 mmol) with 1.1 g of $Cr(CO)_6$ (5 mmol) in benzene for 12 h. The dark red complex was filtered from the mixture and washed with cold benzene. It is air stable and when isolated from benzene solution contains four solvent molecules per molecule of complex, $Cr(O_2C_6Cl_4)_3 \cdot 4C_6H_6$. Crystals of $Cr(O_2C_6Cl_4)_3$ suitable for crystallographic work were grown by recrystallization from a saturated carbon disulfide solution. By this procedure solvated samples of stoichiometry $Cr(O_2C_6Cl_4)_3 \cdot CS_2 \cdot \frac{1}{2}C_6H_6$ were obtained and used in the x-ray investigation.

The cationic complex $[Cr(O_2C_6Cl_4)_3](SbF_6)$ was prepared by addition of a slight molar excess of $AgSbF_6$ in methylene chloride to a similar solution of $Cr(O_2C_6Cl_4)_3$. After a few minutes a gray precipitate of silver metal formed and was separated from the solution by filtration. The complex is lighter in color than the neutral species (orange-red). The ESR spectra of $[Cr(O_2C_6Cl_4)_3](SbF_6)$ were recorded on a Varian E-3 spectrometer. Room temperature spectra were

$$M(CO)_6 + \underset{\text{(structure)}}{\quad} \xrightarrow{C_6H_6} M(O_2C_6Cl_4)_3 \qquad (1)$$

$$M = Cr, Mo, W$$